Dark Matter Searches with sub-keV Germanium Detector

H.B. Li, H.T. Wong

(on behalf of TEXONO collaboration)
Institute of Physics, Academia Sinica, Taipei 11529, Taiwan.

DOI: http://dx.doi.org/10.3204/DESY-PROC-2013-04/li_hau-bin

We report new limits on spin-independent WIMP-nucleon interaction cross-section using 39.5 kg-days of data taken with a p-type point-contact germanium detector of 840 g fiucial mass at the Kuo-Sheng Reactor Neutrino Laboratory. Crucial to this study is the understanding of the selection procedures and, in particular, the bulk-surface events diffentiation at the sub-keV range. The signal-retaining and background-rejecting efficiencies were measured with calibration gamma sources and a novel n-type point-contact germanium detector. Part of the parameter space in cross-section versus WIMP-mass implied by various experiments is probed and excluded.

A kg-scale p-type point-contact germanium detectors (pGe) is sensitive to probe the "low-mass" WIMPs with $m_\chi < 10$ GeV.

We report new results with a pGe of 39.5 kg-days of data at Kuo-Sheng Reactor Neutrino Laboratory (KSNL).

The detector was enclosed by an NaI(Tl) anti-Compton (AC) detector and copper passive shieldings inside a plastic bag purged by nitrogen gas. This set-up was further shielded by, from inside out, 5 cm of copper, 25 cm of boron-loaded polyethylene, 5 cm of steel and 15 cm of lead. This structure was surrounded by cosmic-ray (CR) veto panels made of plastic scintillators read out by photomultipliers. Both AC and CR detectors serve as vetos to reject background and as tags to identify samples for efficiency measurements [1].

Signals from the point-contact is distributed to a fast-timing amplifier which keeps the rise-time information, and to amplifiers at both 6 s and 12 s shaping time which provide energy information. The trigger efficiency was 100% above 300 eVee.

Energy calibration was achieved by the internal X-ray peaks and the zero-energy was defined with the pedestals provided by the random events. The electronics noise-edge is at 400 eVee. A cut-based analysis was adopted. There are three categories of selection criteria: (i) PN cuts diffentiate physics signals from spurious electronic noise; (ii) the AC and CR cuts identify events with activities only at the pGe target; and (iii) the "bulk versus surface events" (BS) cut selects events at the interior. In addition, the efficiencies and suppression factors (ϵ_X,λ_X) for every selection (X=PN,AC,CR,BS) are measured. The physics samples selected these cuts are categorized by "$AC^{-(+)}\otimes CR^{-(+)}\otimes B(S)$", where $AC^{-(+)}$ and $CR^{-(+)}$ represent AC and CR signals in anti-coincidence(coincidence), respectively, while B(S) denote the bulk(surface) samples. The χN candidates would therefore manifest as $AC^-\otimes CR^-\otimes B$ events [1].

The *in situ* doubly-tagged $AC^+\otimes CR^+$ events serve as the physics reference samples, with which the ϵ_{PN} shown in Figure 2 are measured. The majority of the electronics-induced events

above noise-edge are identified($\lambda\sim1$).

The efficiencies for AC and CR selections are measured by the random events to be, respectively, $\epsilon_{\rm AC} > 0.99$ and $\epsilon_{\rm CR} = 0.93$. The suppressions $\lambda_{\rm AC} = 1.0$ above the NaI(Tl) threshold of 20 keVee, $\lambda_{\rm CR} = 0.92$, measured by reference cosmic samples in which the energy depositions at NaI(Tl) are above 20 MeVee.

The surface-electrode of *p*Ge is a lithium-diffused n^+ layer of mm-scale thickness. Partial charge collection in the surface layer gives rise to reduced measureable energy and slower rise-time (τ) in its fast-timing output. The thickness of the S layer was derived to be (1.16±0.09) mm, via the comparison of simulated and observed intensity ratios of γ-peaks from a ^{133}Ba source. This gives rise to a fiducial mass of 840 g.

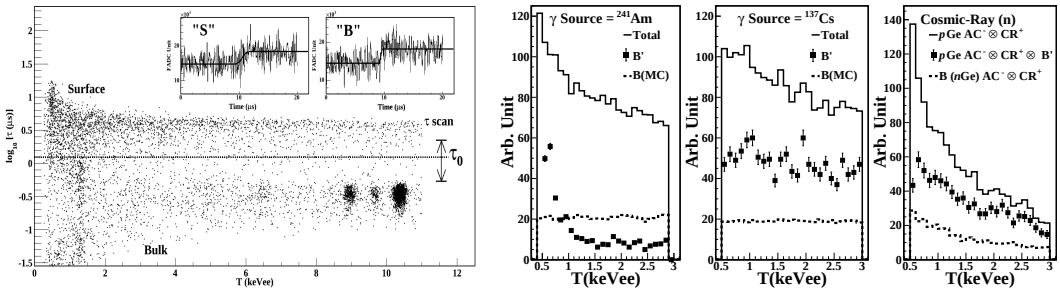

Figure 1: (**left**) log10[τ] versus energy, with τ-scan indicating the range of cut-stability test. Typical B′(S′) pulses at $T\sim700$ eVee are shown. (**right**) The measured Total and B′ spectra from *p*Ge with the surface-rich γ-ray (^{241}Am,^{137}Cs) and bulk-rich cosmic-ray induced neutrons. They are compared to reference B-spectra from simulation and *n*Ge AC$^-\otimes$CR$^+$.

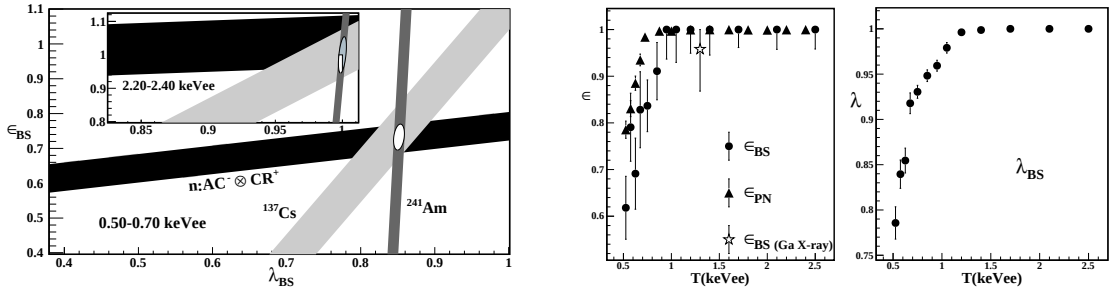

Figure 2: (**left**) Allowed bands at threshold and at a high energy band. (**right**) The measured ($\epsilon_{\rm BS}$,$\lambda_{\rm BS}$) and $\epsilon_{\rm PN}$ as functions of energy. Independent measurement on $\epsilon_{\rm BS}$ with Ga-L X-rays is included.

The $\log_{10}[\tau]$ versus measured energy(T) scatter plot is displayed in Figure 1. Events with τ less(larger) than τ_0 are categorized as B′(S′). The actual bulk(surface) rate are denoted B(S). At T>2.7 keVee where the τ-resolution is better than the separation between the two bands, the conditions B=B′ and S=S′ are justified. At lower energy, (B′,S′) and (B,S) are related by the coupled equations:

$$\mathrm{B}' = \epsilon_{\rm BS}\cdot\mathrm{B} + (1-\lambda_{\rm BS})\cdot\mathrm{S}, \quad \mathrm{S}' = (1-\epsilon_{\rm BS})\cdot\mathrm{B} + \lambda_{\rm BS}\cdot\mathrm{S}, \quad \mathrm{B}+\mathrm{S} = \mathrm{B}'+\mathrm{S}'.$$

The calibration of (ϵ_{BS},λ_{BS}) involves at least two measurements of (B′,S′) where (B,S) are independently known. Three complementary data samples were adopted:

(I) Surface-rich events with γ-ray sources – Calibrations with both low and high energy-sources (^{241}Am at 60 keVee and ^{137}Cs at 662 keVee, respectively) were performed. As displayed in Figure 1, the measured B′- spectra are compared to the reference B derived from simulation.

(II) Bulk-rich events with cosmic-ray induced fast neutrons – A 523 g n-type point-contact germanium (nGe) detector was constructed. The components and dimensions are identical to those of pGe. The surface of nGe is a p+ boron implanted electrode of sub-micron thickness. There are no anomalous surface effects. Data were taken under identical shielding configurations at KSNL. The trigger efficiency was 100% above T=500 eVee, and energy calibration was obtained from the standard internal X-ray lines. The AC$^-\otimes$CR$^+$ condition selects cosmic-ray induced fast neutron events without associated γ-activities, which manifest mostly(85%) as bulk events. Accordingly, the AC$^-\otimes$CR$^+$ spectrum in nGe is taken as the B-reference and compared with those of AC$^-\otimes$CR$^+\otimes$B′ in pGe.

Using calibration data (I) and (II), (ϵ_{BS},λ_{BS}) are measured by solving the coupled equations above. Uncertainties were derived from errors in (B,B′,S′). A consistent ϵ_{BS} is independently measured from Ga-L X-ray peak at 1.3 keVee. As shown in Figure 2.

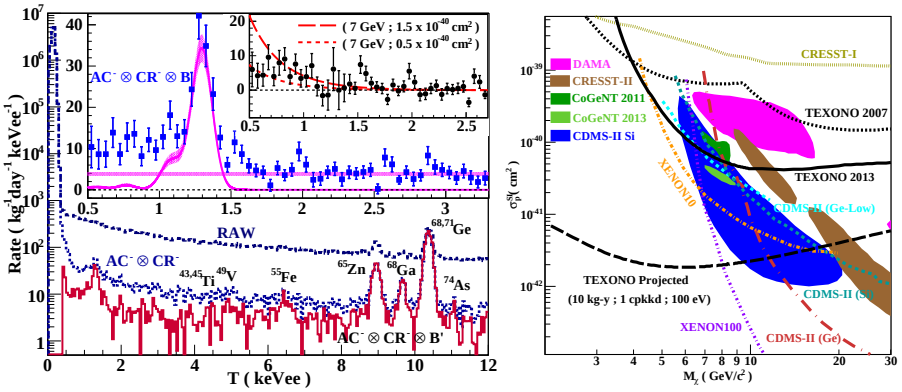

Figure 3: (**left**) Measured energy spectra, showing the raw data and those with AC$^-\otimes$CR$^-$($\otimes$B′) selections. The large inset shows the (ϵ_{BS},λ_{BS})-corrected AC$^-\otimes$CR$^-\otimes$B, with a flat background and L-shell X-ray peaks overlaid. The small inset depicts the residual spectrum superimposed with that due to an allowed (excluded) cross-section at m$_\chi$=7 GeV. (**right**) Exclusion plot of spin-independent χN coupling at 90% confidence level, superimposed with the results from other benchmark experiments.

The raw spectrum as well as those of AC$^-\otimes$CR$^-\otimes$(B′) are depicted in Figure 3. The peaks correspond to known K-shell X-rays from the cosmogenically-activated isotopes. Errors above $T\sim$800 eVee are dominated by statistical uncertainties, while those below have additional contributions due to the BS calibration errors of Figure 2, which increase as (ϵ_{BS},λ_{BS}) deviate from unity at low energy. The analysis threshold is placed at 500 eVee. The stability of B is studied over changes of τ_0 within the τ-scan range of Figure 1. Measurements of B are stable and independent of τ_0. High energy γ-rays from ambient radioactivity produce at electron-recoil background at low energy. This, together with the L-shell X-ray lines predicted by the higher energy K-peaks, are subtracted from AC$^-\otimes$CR$^-\otimes$B.

Constraints on $\sigma^{\rm SI}_{\chi \rm N}$ are derived via the "binned Poisson" method [2] with conventional astrophysical models [3] (local density of 0.3 GeV/cc and Maxwellian velocity distribution with υ_0=220 km/s and υ_{esc}=544 km/s). The quenching function in Ge is derived with the TRIM software.

Exclusion plot of $\sigma^{\rm SI}_{\chi \rm N}$ versus $\rm m_\chi$ at 90% confidence level is displayed in Figure 3. Bounds from other benchmark experiments are superimposeds [4, 5, 6, 7].

We note that an excess remains in the sub-keV region not yet accounted for in this analysis, the understanding of which is the theme of our on-going investigations.

References

[1] H.T. Wong, Mod. Phys. Lett. **A 23**, 1431 (2008). S.T. Lin *et al.*, Phys. Rev. **D 79**, 061101(R) (2009) H.B. Li *et al.*, Phys. Rev. Lett. **90**, 131802 (2003); H.T. Wong *et al.*, Phys. Rev. **D 75**, 012001 (2007); M. Deniz *et al.*, Phys. Rev. **D 81**, 072001 (2010).

[2] C. Savage et al., JCAP **04**, 010 (2009).

[3] M. Drees and G. Gerbier, Review of Particle Physics Phys. Rev. **D 86**, 289 (2012), and references therein.

[4] C.E. Aalseth *et al.*, Phys. Rev. Lett. **101**, 251301 (2008); C.E. Aalseth *et al.*, Phys. Rev. Lett. **106**, 131301 (2011); C.E. Aalseth *et al.*, Phys. Rev. Lett. **107**, 141301 (2011); C.E. Aalseth *et al.*, Phys. Rev. **D 88**, 012002 (2013).

[5] D.S. Akerib *et al.*, Phys. Rev. **D 82**, 122004 (2010); Z. Ahmed *et al.*, Phys. Rev. Lett. **106**, 131302 (2011); J. Angle *et al.*, Phys. Rev. Lett. **107**, 051301 (2011); E. Aprile *et al.*, Phys. Rev. Lett. **109**, 181301 (2012); Z. Ahmed *et al.*, [arXiv:1203.1309 [astro-ph.CO]]

[6] R. Bernabei *et al.*, Eur. Phys. J. **C 67**, 39 (2010); M. Felizardo *et al.*, Phys. Rev. Lett. **108**, 201302 (2012); G. Angloher *et al.*, Eur. Phys. J. **C 72**, 1971 (2012); S. Archambault *et al.*, Phys. Lett. **B 711**, 153 (2012).

[7] D. Hooper, Phys. Dark Univ. **1**, 1 (2012); C. Kelso, D. Hooper, and M.R. Buckley, Phys. Rev. **D 85**, 043515 (2012).